

A.I. Aghazade<sup>1</sup>, E.N. Orujlu<sup>2</sup>, Z.E. Salimov<sup>2</sup>, A.N. Mammadov<sup>1,3</sup>, M.B. Babanly<sup>1</sup>

## Experimental investigation of the solid phase equilibria at 300 K in the SnBi<sub>2</sub>Te<sub>4</sub>-PbBi<sub>2</sub>Te<sub>4</sub>-Bi<sub>2</sub>Te<sub>3</sub> system

<sup>1</sup>M. Nagiyev Institute of Catalysis and Inorganic Chemistry, Baku, Azerbaijan

<sup>2</sup>Azerbaijan State Oil and Industry University, Baku, Azerbaijan

<sup>3</sup>Azerbaijan Technical University, Baku, Azerbaijan, [aytenagazade94@gmail.com](mailto:aytenagazade94@gmail.com), [elnur.oruclu@yahoo.com](mailto:elnur.oruclu@yahoo.com)

The phase equilibria of the SnBi<sub>2</sub>Te<sub>4</sub>-PbBi<sub>2</sub>Te<sub>4</sub>-Bi<sub>2</sub>Te<sub>3</sub> system were experimentally studied using differential thermal analysis (DTA), X-ray diffraction (XRD), and scanning electron microscopy (SEM) techniques. According to the experimental results, the isothermal section of the system at 300 K were constructed and 4 single-phase and 3 two-phase regions were identified. It was shown that along with previously confirmed SnBi<sub>2</sub>Te<sub>4</sub>-PbBi<sub>2</sub>Te<sub>4</sub> and SnBi<sub>4</sub>Te<sub>7</sub>-PbBi<sub>4</sub>Te<sub>7</sub> sections, SnBi<sub>6</sub>Te<sub>10</sub>-PbBi<sub>6</sub>Te<sub>10</sub> section forms continuous series of solid solutions with a tetradymite-type layered structure. Lattice parameters of solid solutions were determined by full-profile Rietveld refinements and results show that both *a* and *c* parameters increase linearly with the Pb concentration according to Vegard's law. This study can help elucidate the phase equilibria of the SnTe-PbTe-Bi<sub>2</sub>Te<sub>3</sub> pseudo-ternary system which provides important information for the design of new tetradymite-type layered phases with topological insulator and thermoelectric properties.

**Keywords:** SnBi<sub>2</sub>Te<sub>4</sub>-PbBi<sub>2</sub>Te<sub>4</sub>-Bi<sub>2</sub>Te<sub>3</sub> system, SnBi<sub>6</sub>Te<sub>10</sub>-PbBi<sub>6</sub>Te<sub>10</sub> section, solid phase equilibria, topological insulators, thermoelectric materials.

Received 24 May 2023; Accepted 5 September 2023.

## Introduction

Bismuth and antimony-based chalcogenides which have tetradymite-type layered structures have received intensive research attention world-widely in the past decades owing to the need for new materials for next-generation technologies [1-5]. These layered chalcogenides were among the most studied and promising materials for thermoelectric power generation from the 50s of the last century [6-8] and experimental verification of topological insulating properties – a new state of quantum matter made these materials even more attractive for researchers around the world [9-15]. Particularly, homologues series of layered ternary compounds were found in the A<sup>IV</sup>-Sb(Bi)-Te ternary systems where A<sup>IV</sup> is Sn, Ge, and Pb elements sparked wide interest in the research community due to both their fundamental scientific interest and the opportunities they offer for observing novel electronic phenomena [16-23].

Creating new multicomponent functional materials is mainly based on the phase equilibria data and thermodynamic properties of the relevant systems [24-29].

The SnTe-PbTe-Bi<sub>2</sub>Te<sub>3</sub> pseudo-ternary system is one key system in terms of having tetradymite-type layered phases. Since boundary pseudo-binary systems form ternary compounds with the same general stoichiometric formula, this pseudo-ternary system can form a series of solid solutions which is important for the optimization of the desired properties.

So far, boundary binary phase relations in SnTe-PbTe-Bi<sub>2</sub>Te<sub>3</sub> pseudo-ternary system has been well studied [30-39]. The latest study on the SnTe-Bi<sub>2</sub>Te<sub>3</sub> section [38] by us described the existence of three tetradymite-type layered intermediate compounds - SnBi<sub>2</sub>Te<sub>4</sub>, SnBi<sub>4</sub>Te<sub>7</sub>, SnBi<sub>6</sub>Te<sub>10</sub> in the 50-100 mol% Bi<sub>2</sub>Te<sub>3</sub> range. Similarly, we described the formation of only three tetradymite-type layered ternary compounds, namely PbBi<sub>2</sub>Te<sub>4</sub>, PbBi<sub>4</sub>Te<sub>7</sub>, and PbBi<sub>6</sub>Te<sub>10</sub> in the PbTe-Bi<sub>2</sub>Te<sub>3</sub> system [39]. The electrical and heat transfer properties of Sn<sub>1-x</sub>Pb<sub>x</sub>Bi<sub>2</sub>Te<sub>4</sub>

series were studied in [40]. The phase relations of  $\text{SnBi}_2\text{Te}_4\text{-PbBi}_2\text{Te}_4$  and  $\text{SnBi}_4\text{Te}_7\text{-PbBi}_4\text{Te}_7$  systems was studied in [27]. It is worth mentioning that up to now, no experimental information on the phase diagram of the  $\text{SnTe-PbTe-Bi}_2\text{Te}_3$  pseudo-ternary system is available in the literature despite above mentioned ternary compounds have been scarcely studied to a large extent as a 3D topological insulator, and thermoelectric materials.

In this perspective, the present work is aiming to determine the solid-phase equilibria of the  $\text{SnBi}_2\text{Te}_4\text{-PbBi}_2\text{Te}_4\text{-Bi}_2\text{Te}_3$  system at 300 K within the framework of an ongoing project for investigating the phase equilibria in the  $\text{SnTe-PbTe-Bi}_2\text{Te}_3$  pseudo-ternary system.

## I. Experimental Details

Alloys of the title system were synthesized from binary  $\text{PbTe}$ ,  $\text{SnTe}$ , and  $\text{Bi}_2\text{Te}_3$  initial compounds. In order to synthesize initial compounds, stoichiometric amounts of pure tin, lead, bismuth, and tellurium (99.999%, Alfa Aesar, and Sigma-Aldrich) were weighed and melted together in vacuum-sealed ( $10^{-2}$  Pa) quartz tubes at temperatures 30-40 K above their melting point and then identified using DTA and XRD methods.

The nominal compositions of alloys were selected on several cross-sections as well as specific phase regions of the  $\text{SnBi}_2\text{Te}_4\text{-PbBi}_2\text{Te}_4\text{-Bi}_2\text{Te}_3$  concentration triangle to study phase equilibria in the whole phase diagram. The weight of each sample was about 0.5 g. Predetermined amounts of initial compounds were weighed and melted together in a furnace at 1100 K for 5 h and then quenched in ice water. The alloys were annealed at 800 K for 1000 hours.

Identification of phase alloys was performed with DTA using the LINSEIS HDSC PT1600 system (accuracy  $\pm 2$  K) with a heating rate of 10 K/min. XRD analysis was carried out on Bruker D2 PHASER diffractometer using  $\text{CuK}\alpha_1$  radiation within the scanning range of  $2\theta = 5\div 75$ . X'pert Highscore Plus and Match 3! Crystal Impact software was used for the determination of lattice

parameters and pattern indexing. The micrographs were received using the Tescan Vega 3 SBH Scanning Electron Microscope equipped with Thermo Scientific Ultra Dry Compact EDS detector.

## II. Results and Discussion

25 alloys were prepared to construct the isothermal section at 300 K in the  $\text{SnBi}_2\text{Te}_4\text{-PbBi}_2\text{Te}_4\text{-Bi}_2\text{Te}_3$  system. In our previous work [27], phase equilibria in the  $\text{SnBi}_2\text{Te}_4\text{-PbBi}_2\text{Te}_4$  and  $\text{SnBi}_4\text{Te}_7\text{-PbBi}_4\text{Te}_7$  sections were already investigated in detail. It was revealed that both sections of the title system form continuous series of solid solutions with a tetradymite-type structure.

In order to determine phase equilibria in the  $\text{SnBi}_6\text{Te}_{10}\text{-PbBi}_6\text{Te}_{10}$  section, annealed alloys with compositions of 20, 40, 60, and 80 mol%  $\text{PbBi}_6\text{Te}_{10}$  were studied by the powder XRD and DTA methods. Fig. 1 shows the XRD results of these alloys. It is clear from the comparison of the diffractograms that the diffraction patterns of all intermediate compositions are qualitatively similar to the initial ternary compounds and alloys have typical tetradymite-type layered diffraction patterns. An analysis of these XRD results confirms that all the reflection peaks of the intermediate alloys can be indexed to the rhombohedral unit cell (hexagonal axis, space group  $R\bar{3}m$ ) and no remarkable impure phases – initial or other compounds are observed. As the concentration of lead increases in alloys, the peaks shift to lower angles which is characteristic of continuous series of solid solutions. This small shift can be attributed to the small differences between the atomic radii of tin and lead.

The lattice constants of the alloys are calculated by the Rietveld technique and obtained results for  $\text{Sn}_{1-x}\text{Pb}_x\text{Bi}_6\text{Te}_{10}$  alloys including previously studied  $\text{Sn}_{1-x}\text{Pb}_x\text{Bi}_2\text{Te}_4$  and  $\text{Sn}_{1-x}\text{Pb}_x\text{Bi}_4\text{Te}_7$  alloys as well as initial ternary compounds are summarized in Table 1. The calculated values of lattice constants for initial ternary compounds –  $\text{SnBi}_2\text{Te}_4$ ,  $\text{SnBi}_4\text{Te}_7$ ,  $\text{SnBi}_6\text{Te}_{10}$ ,  $\text{PbBi}_2\text{Te}_4$ ,  $\text{PbBi}_4\text{Te}_7$ , and  $\text{PbBi}_6\text{Te}_{10}$  are in good agreement with those

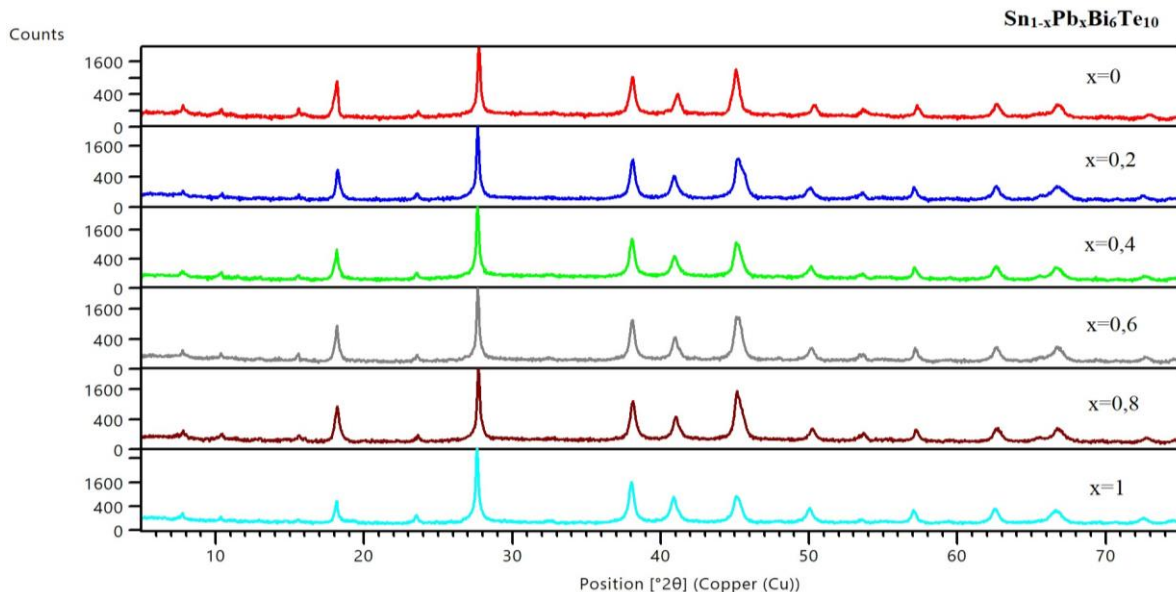
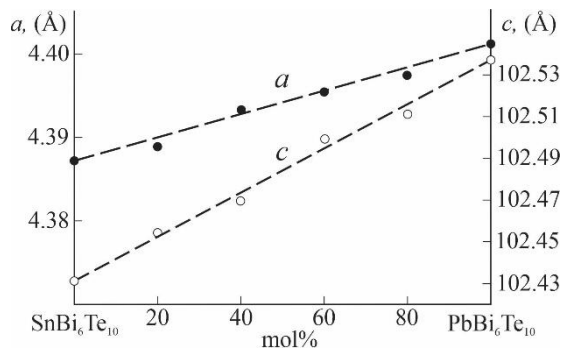


Fig. 1. The XRD patterns of alloys of the  $\text{SnBi}_6\text{Te}_{10}\text{-PbBi}_6\text{Te}_{10}$  section.

**Table 1.**

Crystal structure parameters of some phases

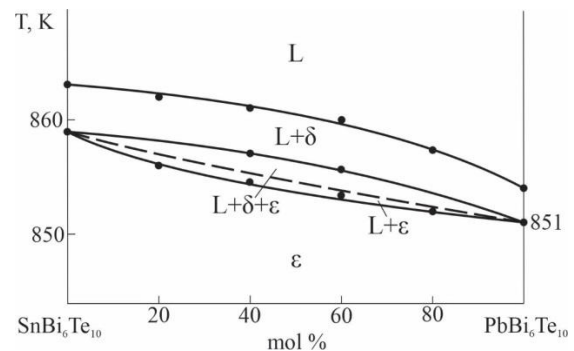
Composition, mol%	Crystal system	Space group	Lattice constants, Å		Ref.
			<i>a</i>	<i>c</i>	
$\text{SnBi}_2\text{Te}_4$	rhombohedral	<i>R-3m</i>	4.40388(3)	41.6015(4)	[27]
20 mol% $\text{PbBi}_2\text{Te}_4$	rhombohedral	<i>R-3m</i>	4.4102(2)	41.625(4)	[27]
40 mol% $\text{PbBi}_2\text{Te}_4$	rhombohedral	<i>R-3m</i>	4.4198(3)	41.655(2)	[27]
60 mol% $\text{PbBi}_2\text{Te}_4$	rhombohedral	<i>R-3m</i>	4.4263(2)	41.673(4)	[27]
80 mol% $\text{PbBi}_2\text{Te}_4$	rhombohedral	<i>R-3m</i>	4.4304(3)	41.695(3)	[27]
$\text{PbBi}_2\text{Te}_4$	rhombohedral	<i>R-3m</i>	4.4385(6)	41.733(7)	[27]
$\text{SnBi}_4\text{Te}_7$	trigonal	<i>P-3m1</i>	4.3998(2)	23.981(3)	[27]
25 mol% $\text{PbBi}_4\text{Te}_7$	trigonal	<i>P-3m1</i>	4.4052(3)	23.964(2)	[27]
50 mol% $\text{PbBi}_4\text{Te}_7$	trigonal	<i>P-3m1</i>	4.4107(3)	23.938(4)	[27]
75 mol% $\text{PbBi}_4\text{Te}_7$	trigonal	<i>P-3m1</i>	4.4152(4)	23.914(2)	[27]
$\text{PbBi}_4\text{Te}_7$	trigonal	<i>P-3m1</i>	4.4233(4)	23.879(7)	[27]
$\text{SnBi}_6\text{Te}_{10}$	rhombohedral	<i>R-3m</i>	4.3873(8)	102.431(1)	This work
20 mol% $\text{PbBi}_6\text{Te}_{10}$	rhombohedral	<i>R-3m</i>	4.3881(5)	102.455(4)	This work
40 mol% $\text{PbBi}_6\text{Te}_{10}$	rhombohedral	<i>R-3m</i>	4.3934(2)	102.472(3)	This work
60 mol% $\text{PbBi}_6\text{Te}_{10}$	rhombohedral	<i>R-3m</i>	4.3956(3)	102.499(6)	This work
80 mol% $\text{PbBi}_6\text{Te}_{10}$	rhombohedral	<i>R-3m</i>	4.3975(3)	102.513(4)	This work
$\text{PbBi}_6\text{Te}_{10}$	rhombohedral	<i>R-3m</i>	4.4012(5)	102.538(2)	[39]


**Fig. 2.** Concentration dependence of lattice parameters of  $\text{Sn}_{1-x}\text{Pb}_x\text{Bi}_6\text{Te}_{10}$  alloys.

reported in [32,34,35] confirm the good accuracy of the present calculations. Besides, lattice parameters vary almost linearly with a composition according to Vegard's law (Fig. 2). These results allow us to conclude the successful formation of continuous solid solutions in the whole concentration range in the  $\text{SnBi}_6\text{Te}_{10}\text{-PbBi}_6\text{Te}_{10}$  section.

The combined results of DTA, XRD, and SEM measurements were used to construct a polythermal section  $\text{SnBi}_6\text{Te}_{10}\text{-PbBi}_6\text{Te}_{10}$  of the phase diagram. As seen from Fig. 3, this section is entirely located in the liquidus surface of the  $\delta$ -phase which is a solid solution with the general formula of  $\text{Sn}_{1-x}\text{Pb}_x\text{Bi}_4\text{Te}_7$ . Therefore, this phase initially crystallizes from the melt. At the next stage of crystallization,  $\text{L}+\delta\leftrightarrow\epsilon$  (859-851 K) monovariant peritectic reaction occurs, which leads to formation of a homogeneous  $\epsilon$ -phase ( $\text{Sn}_{1-x}\text{Pb}_x\text{Bi}_6\text{Te}_{10}$ ).

Thus, all 3 studied polythermal sections ( $\text{SnBi}_2\text{Te}_4\text{-PbBi}_2\text{Te}_4$  [27],  $\text{SnBi}_4\text{Te}_7\text{-PbBi}_4\text{Te}_7$  [27],  $\text{SnBi}_6\text{Te}_{10}\text{-PbBi}_6\text{Te}_{10}$ ) on which continuous series of solid solutions are formed, are not quasi-binary due to the incongruent melting of the initial ternary compounds. However, in the subsolidus region, all these sections are stable. The


**Fig. 3.** T-x diagram of the  $\text{SnBi}_6\text{Te}_{10}\text{-PbBi}_6\text{Te}_{10}$  section.

crystallization processes in all these sections and the general form of their T-x diagrams are qualitatively the same. At the first stage, primary crystallization of the adjacent more refractory phase is observed, and then it enters into a peritectic reaction with the melt to form the final product ( $\gamma$ -,  $\delta$ - or  $\epsilon$ -phase).

According to the experimental data and literature data [27], a solid-phase equilibria diagram of the  $\text{SnBi}_2\text{Te}_4\text{-PbBi}_2\text{Te}_4\text{-Bi}_2\text{Te}_3$  system at 300 K temperature was constructed (Fig. 4.) As can be seen, the system consists of the  $\gamma$ -,  $\delta$ -, and  $\epsilon$ -fields, which represent continuous solid solutions formed on the  $\text{SnBi}_2\text{Te}_4\text{-PbBi}_2\text{Te}_4$ ,  $\text{SnBi}_4\text{Te}_7\text{-PbBi}_4\text{Te}_7$ , and  $\text{SnBi}_6\text{Te}_{10}\text{-PbBi}_6\text{Te}_{10}$  sections, respectively.  $\beta$ -phase reflects the solubility based on the  $\text{Bi}_2\text{Te}_3$  binary compound.

In order to confirm the existence of different phase regions in the  $\text{SnBi}_2\text{Te}_4\text{-PbBi}_2\text{Te}_4\text{-Bi}_2\text{Te}_3$  system, selected alloys inside the concentration triangle were studied by powder XRD and SEM methods. The results are presented in Fig. 5. In all diffractograms, the diffraction lines belonging to different phases are distinguished by different symbols. Fig. 5(a) and (b) show the XRD patterns and SEM micrographs of alloy #1. As can be seen, the XRD pattern contains diffraction lines of  $\gamma$ -, and  $\delta$ -phases, dark gray and light gray regions

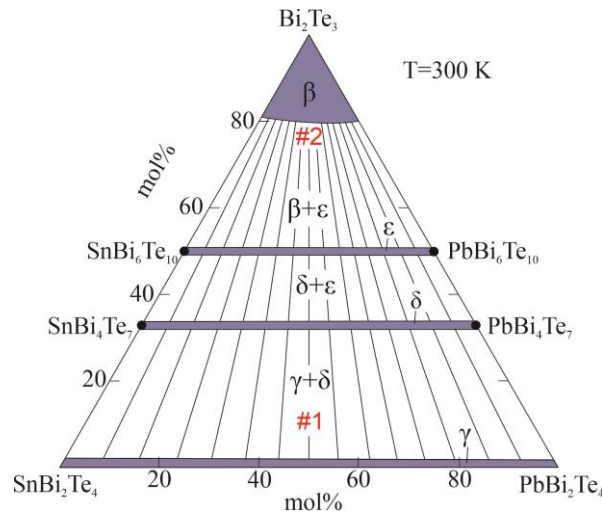


Fig. 4. Isothermal section of the  $\text{SnBi}_2\text{Te}_4$ - $\text{PbBi}_2\text{Te}_4$ - $\text{Bi}_2\text{Te}_3$  system.

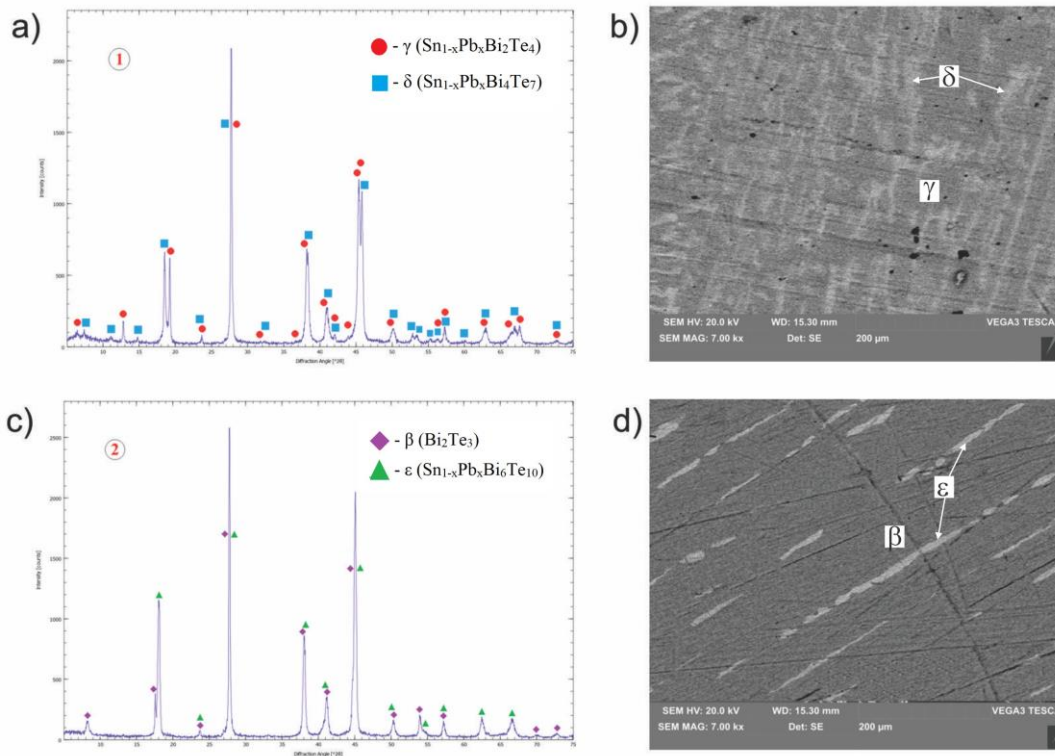


Fig. 5. The XRD patterns and SEM images of alloys #1 (a and b) and #2 (c and d) are in Fig. 4.

belonging to these phases can easily distinguished in the SEM images as well. Alloy #2 is in the  $\beta+\epsilon$  -two-phase region, and the XRD pattern and SEM micrograph are shown in Fig. 5(c) and (d) confirm this.

## Conclusion

The solid-phase equilibria diagram of the  $\text{SnBi}_2\text{Te}_4$ - $\text{PbBi}_2\text{Te}_4$ - $\text{Bi}_2\text{Te}_3$  system at 300K was investigated by means of powder XRD, DTA, and SEM methods. The formation of continuous solid solutions with a tetradymite-type layered structure was revealed in 3 sections -  $\text{SnBi}_2\text{Te}_4$ - $\text{PbBi}_2\text{Te}_4$ ,  $\text{SnBi}_4\text{Te}_7$ - $\text{PbBi}_4\text{Te}_7$ , and  $\text{SnBi}_6\text{Te}_{10}$ - $\text{PbBi}_6\text{Te}_{10}$  of the studied system. Besides, there is a solid solubility based on the initial binary compound

$\text{Bi}_2\text{Te}_3$ . Lattice parameters of solid solutions were refined via the Rietveld technique. Overall, the 300 K isothermal section of this system contains 4 single-phase and 3 two-phase regions. The obtained solid solutions and newly characterized phases with tetradymite-type structures are of great interest as topological insulators and thermoelectric materials.

## Acknowledgements

The work was supported by the Azerbaijan Science Foundation - Grant № AEF-MCG-2022-1(42)-12/10/4-M-10.

**Aghazade A.I.** – Ph.D. student, Researcher, M. Nagiyev Institute of Catalysis and Inorganic Chemistry;  
**Orujlu E.N.** – Ph.D. on Chemistry, Azerbaijan State Oil and Industry University;  
**Salimov Z.E.** – Ph.D. on Chemistry, Azerbaijan State Oil and Industry University;

**Mammadov A.N.** – doctor of chemical sciences, professor, M. Nagiyev Institute of Catalysis and Inorganic Chemistry;  
**Babanly M.B.** – doctor of chemical sciences, professor, Corresponding member of ANAS, M. Nagiyev Institute of Catalysis and Inorganic Chemistry.

- [1] N. Virk, O. Yazyev, *Dirac fermions at high-index surfaces of bismuth chalcogenide topological insulator nanostructures*, Sci Rep, 6(1), 20220 (2016); <https://doi.org/10.1038/srep20220>.
- [2] L.D. Ivanova, I.Y. Nikhezina, Y.V. Granatkina, V.A. Dudarev, S. A. Kichik, A.A. Mel'nikov, *Thermoelements from antimony- and bismuth-chalcogenide alloys*, Semiconductors, 51(8), 986 (2017); <https://doi.org/10.1134/S1063782617080140>.
- [3] G.S. Hegde, A.N. Prabhu, *A Review on Doped/Composite Bismuth Chalcogenide Compounds for Thermoelectric Device Applications: Various Synthesis Techniques and Challenges*. J. Electron. Mater., 51, 2014 (2022); <https://doi.org/10.1007/s11664-022-09513-x>.
- [4] R. Golovchak, J. Plummer, A. Kovalskiy, Y. Holovchak, T. Ignatova, A. Trofe, B. Mahlovanyi, J. Cebulski, P. Krzeminski, Y. Shpotyuk, C. Boussard-Pledel, B. Bureau, *Phase-change materials based on amorphous equichalcogenides*, Sci Rep, 13, 2881 (2023); <https://doi.org/10.1038/s41598-023-30160-7>.
- [5] W-C. Lin, Y-C. Yang, H-Y. Tuan, *Ternary chalcogenide anodes for high-performance potassium-ion batteries and hybrid capacitors via composition-mediated bond softening and intermediate phase*, Energy Storage Materials, 51, 38 (2022); <https://doi.org/10.1016/j.ensm.2022.06.010>.
- [6] H.J. Goldsmid, R.W. Douglas. *The use of semiconductors in thermoelectric refrigeration*, British Journal of Applied Physics, 5, 386 (1954).
- [7] A.V. Shevelkov. *Chemical aspects of the design of thermoelectric materials*, Russian Chemical Reviews, 77(1), 1 (2008); <https://doi.org/10.1070/RC2008v077n01ABEH003746>.
- [8] G. Tan, M. Ohta, M. G. Kanatzidis. *Thermoelectric power generation: from new materials to devices*, Philosophical Transactions of the Royal Society B, 377(2152), 20180450 (2019); <https://doi.org/10.1098/rsta.2018.0450>.
- [9] X. L. Qi, S. C. Zhang. *Topological insulators and superconductors*, Reviews of Modern Physics, 83, 1057 (2011); <https://doi.org/10.1103/RevModPhys.83.1057>.
- [10] L. Hu, H. Gao, X. Liu H. Xie, J. Shen, T. Zhu, X.Zhaoa, *Enhancement in thermoelectric performance of bismuth telluride based alloys by multi-scale microstructural effects*, Journal of Materials Chemistry. 22, 16484 (2012); <https://doi.org/10.1039/C2JM32916F>.
- [11] H. Zhang, C-X. Liu, X-L. Qi, X. Dai, Z. Fang, S-C. Zhang, *Topological insulators in Bi<sub>2</sub>Se<sub>3</sub>, Bi<sub>2</sub>Te<sub>3</sub> and Sb<sub>2</sub>Te<sub>3</sub> with a single Dirac cone on the surface*, Nature Phys, 5, 438 (2009); <https://doi.org/10.1038/nphys1270>.
- [12] Y.L. Chen, J.G. Analytis, J-H. Chu, Z.K. Liu, S-K. Mo, X.L. Qi, H.J. Zhang, D.H. Lu, X. Dai, Z. Fang, S.C. Zhang, I.R. Fisher, Z. Hussain, Z-X. Shen, *Experimental Realization of a Three-Dimensional Topological Insulator, Bi<sub>2</sub>Te<sub>3</sub>*, Science, 325, 178 (2009); <https://doi.org/10.1126/science.1173034>.
- [13] L. Zhao, H. Deng, I. M. Begliarbekov, Z. Chen, E. Andrade, E. Rosenthal, A. Pasupathy, V. Oganessian, L. Krusin-Elbaum, *Emergent surface superconductivity in the topological insulator Sb<sub>2</sub>Te<sub>3</sub>*, Nat Commun, 6, 8279 (2015); <https://doi.org/10.1038/ncomms9279>.
- [14] C. Lamuta, A. Cupolillo, A. Politano, Z.S. Aliev, M.B. Babanly, E.V. Chulkov, L. Pagnotta, *Indentation fracture toughness of single-crystal Bi<sub>2</sub>Te<sub>3</sub> topological insulators*, Nano Research, 9, 1032 (2016); <https://doi.org/10.1007/s12274-016-0995-z>.
- [15] R. Flammini, S. Colonna, C. Hogan, S.K. Mahatha, M. Papagno, A. Barla, P.M. Sheverdyayeva, P. Moras, Z.S. Aliev, M.B. Babanly, E.V. Chulkov, C. Carbone, F. Ronci, *Evidence of  $\beta$ -antimonene at the Sb/Bi<sub>2</sub>Se<sub>3</sub> interface*. Nanotechnology, 29(6), 065704 (2018); <https://doi.org/10.1088/1361-6528/aaa2c4>.
- [16] A. Politano, M. Caputo, S. Nappini, F. Bondino, E. Magnano, Z.S. Aliev, M.B. Babanly, A. Goldoni, G. Chiarello, E. V. Chulkov, *Exploring the Surface Chemical Reactivity of Single Crystals of Binary and Ternary Bismuth Chalcogenides*, J. Phys. Chem. C, 118(37), 21517 (2014); <https://doi.org/10.1021/jp506444f>.
- [17] L-L. Wang, *Highly tunable band inversion in AB<sub>2</sub>X<sub>4</sub> (A=Ge, Sn, Pb; B=As, Sb, Bi; X=Se, Te) compounds*, Phys. Rev. Materials, 6, 094201 (2022); <https://doi.org/10.1103/PhysRevMaterials.6.094201>.
- [18] A. Saxena, N.K. Karn, M.M. Sharma, V.P.S. Awana, *Detailed structural and topological analysis of SnBi<sub>2</sub>Te<sub>4</sub> single crystal*, J. Phys. Chem. Solids, 174, 111169 (2022); <https://doi.org/10.1016/j.jpcs.2022.111169>.
- [19] M.G. Vergniory, T.V. Menshchikova, S.V. Eremeev, E.V. Chulkov, *Bulk and surface electronic structure of SnBi<sub>4</sub>Te<sub>7</sub> topological insulator*, Applied Surface Science, 267, 146 (2013); <https://doi.org/10.1016/j.apsusc.2012.08.073>.
- [20] M. Papagno, S. V. Eremeev, J. Fujii, Z. S. Aliev, M. B. Babanly, S. Mahatha, I. Vobornik, N. T. Mamedov, D. Pacile, E. V. Chulkov, *Multiple Coexisting Dirac Surface States in Three-Dimensional Topological Insulator PbBi<sub>6</sub>Te<sub>10</sub>*, ACS Nano, 10(3), 3518 (2016); <https://doi.org/10.1021/acsnano.5b07750>.

- [21] R. Li, G. Liu, Q. Jing, X. Wang, H. Wang, J. Zhang, Y. Ma, *Pressure-induced superconductivity and structural transitions in topological insulator  $\text{SnBi}_2\text{Te}_4$* , *J. Alloys Compd.*, 900, 163371 (2022); <https://doi.org/10.1016/j.jallcom.2021.163371>.
- [22] K. Konstantinou, F.C. Mocanu, J. Akola, *Electron localization in recrystallized models of the  $\text{Ge}_2\text{Sb}_2\text{Te}_3$  phase-change memory material*, *Phys. Rev. B*, 106, 184103 (2022); <https://doi.org/10.1103/PhysRevB.106.184103>.
- [23] M. Nurmamat, K. Okamoto, S. Zhu, T.V. Menshchikova, I.P. Rusinov, V. O. Korostev, K. Miyamoto, T. Okuda, T. Miyashita, X. Wang, Y. Ishida, K. Sumida, E.F. Schwier, M. Ye, Z.S. Aliev, M.B. Babanly, I.R. Amiraslanov, E.V. Chulkov, K.A. Kokh, O.E. Tereshchenko, K. Shimada, S. Shin, A. Kimura, *Topologically Nontrivial Phase-Change Compound  $\text{GeSb}_2\text{Te}_4$* , *ACS Nano*, 14(7), 9059 (2020); <https://doi.org/10.1021/acsnano.0c04145>.
- [24] M.B. Babanly, E.V. Chulkov, Z.S. Aliev, A.V. Shevelkov, I.R. Amiraslanov, *Phase diagrams in materials science of topological insulators based on metal chalcogenides*, *Russ. J. Inorg. Chem.*, 62, 1703 (2017); <https://doi.org/10.1134/S0036023617130034>.
- [25] S.Z. Imamaliyeva, D.M. Babanly, D.B. Tagiev, M.B. Babanly, *Physicochemical Aspects of Development of Multicomponent Chalcogenide Phases Having the  $\text{Tl}_5\text{Te}_3$  Structure: A Review*, *Russ. J. Inorg. Chem.*, 63, 1704 (2018); <https://doi.org/10.1134/S0036023618130041>.
- [26] E.N. Orujlu, Z.S. Aliev, M.B. Babanly, *The phase diagram of the  $\text{MnTe-SnTe-Sb}_2\text{Te}_3$  ternary system and synthesis of the iso- and aliovalent cation-substituted solid solutions*, *Calphad*, 76, 102398 (2022); <https://doi.org/10.1016/j.calphad.2022.102398>.
- [27] A.I. Aghazade, *Phase relations and characterization of solid solutions in the  $\text{SnBi}_2\text{Te}_4\text{-PbBi}_2\text{Te}_4$  and  $\text{SnBi}_4\text{Te}_7\text{-PbBi}_4\text{Te}_7$  systems*, *J. Azerb. Chem.*, 3, 75 (2022); <https://doi.org/10.32737/0005-2531-2020-4-53-59>.
- [28] E.N. Orujlu, *Phase relations and characterization of solid solutions in the  $\text{SnSb}_2\text{Te}_4\text{-MnSb}_2\text{Te}_4$  system*, *New Materials, Compounds and Applications*, 4(1), 38 (2020).
- [29] Y. Hattori, Y. Tokumoto, K. Kimoto, K. Edagawa, *Evidences of inner Se ordering in topological insulator  $\text{PbBi}_2\text{Te}_4\text{-PbBi}_2\text{Se}_4\text{-PbSb}_2\text{Se}_4$  solid solutions*, *Sci Rep*, 10, 7957 (2020); <https://doi.org/10.1038/s41598-020-64742-6>.
- [30] K. Adouby, A. Abba Touré, G. Kra, J. Olivier-Fourcade, J-C. Jumas, C. Perez Vicente, *Phase diagram and local environment of Sn and Te:  $\text{SnTe-Bi}$  and  $\text{SnTe-Bi}_2\text{Te}_3$  systems*, *Comptes Rendus de l'Académie Des Sciences - Series IIC - Chemistry*, 3(1), 51 (2000); [https://doi.org/10.1016/s1387-1609\(00\)00105-5](https://doi.org/10.1016/s1387-1609(00)00105-5).
- [31] Cn. Chiu, Cm. Hsu, Sw. Chen, Hj. Wu, *Phase Equilibria of the  $\text{Sn-Bi-Te}$  Ternary System*, *J. Electron. Mater.*, 41, 22 (2012); <https://doi.org/10.1007/s11664-011-1730-x>.
- [32] O.G. Karpinskii, L.E. Shelimova, M.A. Kretova, E.S. Avilov, V.S. Zemskov, *X-ray Diffraction Study of Mixed-Layer Compounds in the Pseudobinary System  $\text{SnTe-Bi}_2\text{Te}_3$* , *Inorganic Materials*, 39, 240 (2003); <https://doi.org/10.1023/A:1022669323255>.
- [33] D. Huang, D. Xia, T. Ye, T. Fujita, *New experimental studies on the phase relationship of the  $\text{Bi-Pb-Te}$  system*, *Materials & Design*, 224, 111384 (2022); <https://doi.org/10.1016/j.matdes.2022.111384>.
- [34] L.E. Shelimova, O.G. Karpinskii, P.P. Konstantinov, E. S. Avilov, M.A. Kretova, I.Yu. Nikhezina, V.S. Zemskov, *Thermoelectric materials based on intermediate phases in the systems formed by chalcogenides of lead and bismuth*, *Inorg. Mater. Appl. Res.*, 1, 83 (2010); <https://doi.org/10.1134/S2075113310020024>.
- [35] B.A. Kuropatwa, H. Kleinke, *Thermoelectric Properties of Stoichiometric Compounds in the  $(\text{SnTe})_x(\text{Bi}_2\text{Te}_3)_y$  System*, *Z. anorg. allg. Chem.*, 638(15) 2640 (2012); <https://doi.org/10.1002/zaac.201200284>.
- [36] O.G. Karpinskii, L.E. Shelimova, E.S. Avilov, M.A. Kretova, V.S. Zemskov, *X-ray Diffraction Study of Mixed-Layer Compounds in the  $\text{PbTe-Bi}_2\text{Te}_3$  System*, *Inorg. Mater.*, 38, 17 (2002); <https://doi.org/10.1023/A:1013639108297>.
- [37] L.E. Shelimova, O.G. Karpinskii, T.E. Svechnikova, E.S. Avilov, M.A. Kretova, V.S. Zemskov, *Synthesis and structure of layered compounds in the  $\text{PbTe-Bi}_2\text{Te}_3$  and  $\text{PbTe-Sb}_2\text{Te}_3$  systems*, *Inorg. Mater.*, 40, 1264 (2004); <https://doi.org/10.1007/s10789-005-0007-2>.
- [38] A.E. Seidzade, E.N. Orujlu, Z.S. Aliev, M.B. Babanly, *New investigation of phase equilibria in the  $\text{SnTe-Bi}_2\text{Te}_3$  system*, 10<sup>th</sup> Rostocker International Conference: "Thermophysical Properties for Technical Thermodynamics" (Rostock, Germany, 2021), P.134.
- [39] I.M. Gojayeva, V.I. Babanly, A.I. Aghazade, E.N. Orujlu, *Experimental reinvestigation of the  $\text{PbTe-Bi}_2\text{Te}_3$  pseudo-binary system*, *J. Azerb. Chem.*, 1(2), 47 (2022); <https://doi.org/10.32737/0005-2531-2022-2-47-53>.
- [40] L. Pan, J. Li, D. Berardan, N. Dragoe, *Transport properties of the  $\text{SnBi}_2\text{Te}_4\text{-PbBi}_2\text{Te}_4$  solid solution*, *J. Solid State Chem.*, 225, 168 (2015); <https://doi.org/10.1016/j.jssc.2014.12.016>.

А.І. Агхазаде<sup>1</sup>, Є.Н. Оруйлу<sup>2</sup>, З.Е. Салімов<sup>2</sup>, А.Н. Маммадов<sup>1,3</sup>, М.Б. Бабанли<sup>1</sup>

## Експериментальне дослідження твердофазної рівноваги у системі $\text{SnBi}_2\text{Te}_4\text{-PbBi}_2\text{Te}_4\text{-Bi}_2\text{Te}_3$ при 300 К

<sup>1</sup>Інститут каталізу та неорганічної хімії імені М. Нагієва, Баку, Азербайджан

<sup>2</sup>Азербайджанський державний університет нафти та промисловості, Баку, Азербайджан

<sup>3</sup>Азербайджанський технічний університет, Баку, Азербайджан, [aytenagazade94@gmail.com](mailto:aytenagazade94@gmail.com), [elnur.oruclu@yahoo.com](mailto:elnur.oruclu@yahoo.com)

Фазові рівноваги системи  $\text{SnBi}_2\text{Te}_4\text{-PbBi}_2\text{Te}_4\text{-Bi}_2\text{Te}_3$  експериментально досліджено методами диференціального термічного аналізу (ДТА), рентгенівської дифракції (РФА) та скануючої електронної мікроскопії (СЕМ). За результатами експерименту побудовано ізотермічний перетин системи при 300 К і виділено 4 однофазні та 3 двофазні області. Показано, що поряд із раніше підтвердженими розрізами  $\text{SnBi}_2\text{Te}_4\text{-PbBi}_2\text{Te}_4$  та  $\text{SnBi}_4\text{Te}_7\text{-PbBi}_4\text{Te}_7$ , розріз  $\text{SnBi}_6\text{Te}_{10}\text{-PbBi}_6\text{Te}_{10}$  утворює суцільний ряд твердих розчинів із шаруватою структурою тетрадимітового типу. Параметри решітки твердих розчинів були визначені повнопрофільним уточненням Рітвельда. Результати показують, що як параметри  $a$ , так і  $c$  зростають лінійно із концентрацією Рb, відповідно до закону Vegarda. Це дослідження може допомогти з'ясувати фазові рівноваги псевдопотрійної системи  $\text{SnTe-PbTe-Bi}_2\text{Te}_3$ , яка надає важливу інформацію для розробки нових шаруватих фаз тетрадимітового типу із топологічним ізолятором і термоелектричними властивостями.

**Ключові слова:** система  $\text{SnBi}_2\text{Te}_4\text{-PbBi}_2\text{Te}_4\text{-Bi}_2\text{Te}_3$ , розріз  $\text{SnBi}_6\text{Te}_{10}\text{-PbBi}_6\text{Te}_{10}$ , твердофазна рівновага, топологічні ізолятори, термоелектричні матеріали.